adsorption time because of blocking of the unoccupied silanol groups by earlier arrivals, in which the overall chain conformation of one end-attached T-PBR chain is not much different from the free chain conformation suggested by Hesselink[22] and Tanaka.[23] Subsequently, the double bonds in butadiene parts of T-PBR chains adsorb on the silanol groups in order to attain an equilibrium state, and finally an adsorbed amount twice as large as that of PBR chains is established for T-PBR chains.

The bound fraction $p$ is sometimes useful to infer the conformation of adsorbed polymer chain. Since the plateau value of $p$ is nearly constant irrespective of polymers, one can imagine that the conformation of adsorbed T-PBR chains is not different from that of adsorbed PBR chains. However, for T-PBR chains their one end is undoubtedly attached to the silica surface due to the high adsorbability of the terminal group. The polymer segments located close to the anchored end adsorb easily on the silica surface since their mobility should be restrained in comparison with that of unadsorbed segments located far from the adsorbed end segment. Therefore, in the equilibrium state T-PBR chains take a conformation consisting of one relative long tail and some short loops as well as trains. On the other hand, the adsorbed PBR chains will take the generally accepted loop–train–tail conformation, where both ends are dangling. The difference between both adsorbed conformations may be explored by the measurement of adsorbed layer thickness. A preliminary ellipsometric study[24] of adsorption of T-PBR and PBR onto a platinum plate from carbon tetrachloride solution showed that the thickness of T-PBR is thicker than that of PBR and the adsorbance of T-PBR is ~1.5 times that of PBR. These ellipsometric data seem to be convenient for more adsorbed polymer on the surface for the T-PBR chains.

The plateau data on $p$ and $\theta$ for T-PBR imply on the order of 300 covered adsorbed segments per chain ($p \sim 0.1$) and on the order of 600 silanol groups per particle; i.e., two molecules are adsorbed on the silica surface if no bridging between different silica particles is assumed. T-PBR chains whose radii of gyration is on the order of 200 Å will be able to wrap around the silica particle well by taking the suggested structure of adsorbed chains.

## Conclusions

High molecular weight polybutadienes terminated with a single very polar group show a different adsorption behavior at the silica surface in carbon tetrachloride as compared with normal polybutadiene. The former has an adsorbed amount and a surface coverage of the silanol groups that are twice as large as the same features in the latter, but the bond fraction $p$ (i.e., the fraction of monomers of adsorbed chains being in contact with the surface) is almost equal for both polymers. This difference is rather speculatively interpreted by taking into account the preferential adsorption of terminal polar groups to the silanol groups over the double bonds in butadiene chains. We wish to emphasize that a chain end terminated with polar groups is very important for the determination of adsorption behavior of polymer chains.

**Registry No.** $SiO_2$, 7631-86-9.

## References and Notes


(1) Vincent, B.; Whittington, S. In *Surface and Colloid Science*; Matijevic, E., Ed.; Plenum: New York, 1981; p 1.
(2) Tadros, Th. F. In *The Effect of Polymers on Dispersion Properties*; Tadros, Th. F., Ed.; Academic: London, 1982; p 1.
(3) Takahashi, A.; Kawaguchi, M. *Adv. Polym. Sci.* **1982**, *46*, 1.
(4) Fleer, G. J.; Lyklema, J. In *Adsorption from Solution at the Solid/Liquid Interface*; Parfitt, G. D., Rochester, C. H., Eds.; Academic: London, 1983; p 153.
(5) Napper, D. H. *Polymeric Stabilization of Colloidal Dispersions*; Academic: London, 1983.
(6) Hadziioannou, G.; Patel, S.; Granick, S.; Tirrell, M. *J. Am. Chem. Soc.* **1986**, *108*, 2869.
(7) Kawaguchi, M.; Oohira, M.; Tajima, M.; Takahashi, A. *Polym. J.* **1980**, *12*, 849.
(8) Bringuier, E.; Vilanove, R.; Gattot, Y.; Selb, J.; Rondelez, F. *J. Colloid Interface Sci.* **1985**, *104*, 95.
(9) Crowl, V. T.; Matati, M. A. *Discuss. Faraday Soc.* **1966**, *42*, 301.
(10) Crowl, V. T. *J. Oil Colour Chem. Assoc.* **1967** *50*, 1023.
(11) Sakai, I.; Nakamae, K.; Ohkawa, T.; Inubushi, H.; Mastumoto, T. *Kobunshi Ronbunshu* **1977**, *34*, 661.
(12) Yoshioka, A.; Komuro, K.; Ueda, A.; Watanabe, H.; Akita, S.; Masuda, T.; Nakajima, A. *Pure Appl. Chem.* **1986**, *53*, 1697.
(13) Kawaguchi, M.; Sano, T.; Takahashi, A. *Polym. J.* **1981**, *13*, 1019.
(14) Kawaguchi, M.; Aoki, M.; Takahashi, A. *Macromolecules* **1983**, *16*, 635.
(15) Little, L. H.; Mathieu, M. V. *Actes Congr. Int. Catal., 2nd* **1960**, 771.
(16) Marshall, K.; Rochester, C. H. *J. Chem. Soc., Faraday Trans. 1* **1975**, *71*, 1754.
(17) Howard, G. J. In *Interfacial Phenomena in Apolar Media*; Eicke, H. F., Parfitt, G. D., Eds.; Dekker: New York, 1987; p 281.
(18) Griffiths, D. M.; Marshall, K.; Rochester, C. H. *J. Chem. Soc., Faraday Trans. 1* **1974**, *70*, 400.
(19) Curthoys, G.; Davydov, V. Ya.; Kiselev, A. V.; Kiselev, S. A.; Kuznetsov, B. V. *J. Colloid Interface Sci.* **1974**, *48*, 58.
(20) Rochester, C. H. *Adv. Colloid Interface Sci.* **1980**, *12*, 43.
(21) Kawaguchi, M.; Kawarabayashi, M.; Takahashi, A., unpublished data.
(22) Hesselink, F. Th. *J. Colloid Interface Sci.* **1975**, *50*, 606.
(23) Tanaka, T. *Macromolecules* **1977**, *10*, 51.
(24) Kawaguchi, M.; Kawarabayashi, M.; Takahashi, A., unpublished data.


# Molecular Rheology of H-Polymers


**T. C. B. McLeish**

*Cavendish Laboratory, Madingley Road, Cambridge CB3 0HE, United Kingdom.*

*Received July 8, 1987*


ABSTRACT: The rheological behavior of branched polymer melts contrasted with that of linear melts motivates a discussion of a molecular model of a melt of H-polymers. Concentrating on the dynamics of the "backbone", we derive and discuss the linear viscoelastic properties in the light of experiments by Roovers.[23] The model is extended to treat nonlinear deformations, with path-length extension treated in a self-consistent way, and compared with rheological behavior of branched LDPE.


## Introduction

The primitive path or tube model of polymer melts as developed by Doi and Edwards[1–4] has met with considerable success when applied to the dynamics of linear polymers.[5–7] The extension of the theory to star polymers has been made[8,9,20] and is in accord with both numerical[10]

0024-9297/88/2221-1062$01.50/0 

and experimental[9] data on the diffusion and viscosity of stars.

Industrially, more complex branched polymers, such as LDPE, are very important. This has motivated many rheological studies[12-14] which consistently show behavior different from that of linear polymers. In particular we note the following: (1) The viscosity/molecular weight relationship of branched polymers is faster than power law.[16] (2) They are less strain softening in step strain and can be strain hardening.[15] (3) In steady flow they can be strain hardening, especially in extension.[12] (4) In capillary flow extrusion they exhibit different forms of instability than those of linear melts and in particular do not show the throughput discontinuities of linear melts.[17,7] (5) In converging flow from a reservoir into a capillary[18,19,34] they follow "wine glass" shaped streamlines and develop a large rotating ring vortex in contrast to linear polymers, which follow streamlines resembling those of a newtonian liquid, even at quite large Deborah numbers.

Though a detailed study has not been made, Pearson and Helfand[21] report that under large strains the behavior of stars is similar to that of linear polymers. This is understandable in terms of the tube model because, like linear polymers, each arm of a star is able to equilibrate its own contour length on a time scale much faster than the diffusion of the molecule as a whole. It seems that interesting new rheology occurs when there is more than one branch point per molecule. This situation implies a fraction of chain segments "trapped" between branch points. Their orientation and contribution to the viscoelastic stress will follow a dynamics different from that of the free arms.

Recently there have been studies of the linear viscoelasticity of well-characterized branched polymers by Roovers and Graessley[22] on combs and by Roovers[23] on H's. The H-polymer makes an appealing subject of study both experimentally[23] and theoretically, as first suggested by Marrucci,[24] because it is the simplest species containing some chain length between branch points. In this paper we consider how the tube model may be extended to this example.

## The Model

We consider an H-polymer melt, in which each part of the molecule is highly entangled with its environment. The greatest constraint on the motion of a molecule comes from its branch points, for they may only take a diffusive step when one of the free arms retraces to the branch point. It does this with a probability varying inverse exponentially with the molecular weight of the arm. This is the dominant process in the diffusion of entangled star molecules[8,9,11,24,25] and leads to a diffusion constant for three-arm stars of[25]

$$D \sim kT(M_a/M_e)^{-\alpha} \exp(-\nu M_a/M_e) \quad (1)$$

Here $M_a$ is the molecular weight of the star arm and $M_e$ the entanglement molecular weight. Values of $\alpha$ and $\nu$ vary between authors as described by Klein,[25] but for concreteness we take $\alpha = {}^3/_2$ which comes from the solution to the first-passage Smolochowski problem considered by Pearson and Helfand. Experimentally a universal value of $\nu = 0.6$ has been reported for stars,[9] though there has been some discussion of this point.[21] Doi used a value of $\nu = {}^3/_2$ in the path-length potential to investigate path-length fluctuations in linear polymers.[28] This value comes from treating the primitive path as a Gaussian chain in free space. Pearson and Helfand,[21] however, argue that the presence of entanglements is essential in evaluating the entropy change associated with extending the primitive path. They performed a calculation of the distribution of nonentangled primitive path lengths on a lattice of coordination number $q$ and found $\nu = q(q-2)/8(q-1)$. The Doi result therefore requires an effective coordination number of $q \cong 13$, and the experimental results of Pearson and Helfand require $q \cong 6$. The theoretical difficulty of the lattice approach lies in determining $q$ for an off-lattice real polymer. We add here that the value of $\nu$ for H-polymers calculated from the plot of Figure 3 (assuming that this correctly gives us the exponential term in $\eta_0$), and applying the model outlined below, is $\nu = 1.2$.

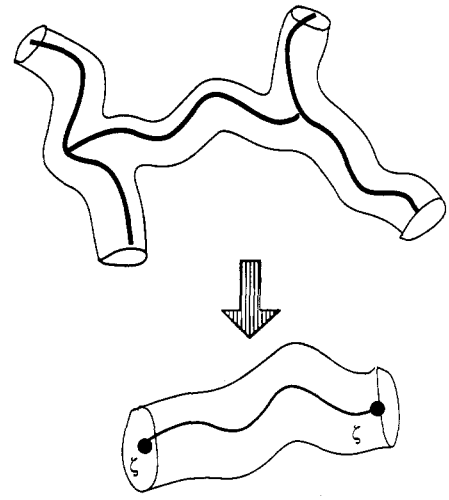


**Figure 1.** Renormalization of an H-polymer in a tube as two connected point diffusers.

When two three-arm stars are "joined up" to make an H-polymer, the longest relaxation process must be the reptation of the "backbone" (providing it is long enough to be entangled). The monomeric friction coefficient along the backbone can be ignored relative to the contribution from the branch points, each of which can be thought of as a bead with friction coefficient $\zeta$, where $\zeta$ is related to $D$ in (1) via an Einstein relation:

$$\zeta \sim (M_a/M_e)^{3/2} \exp(\nu M_a/M_e) \quad (2)$$

In a stress relaxation experiment, all the stress contribution from the arms must be completely removed before the branch point can take one diffusive step, so the stress behavior under deformation will be dominated by the backbone at long times. We are left with a model of the entangled H-polymer which looks like a Rouse chain in a tube with its friction concentrated at its end points, as illustrated in Figure 1. A branch point may make a diffusive step either toward the other, when it must follow the orientation of the tube, or away from it, when the orientation of the new tube segment then created is assumed to be random (in modified versions of reptation theories it may be necessary to adjust this assumption[27]).

Two caveats should be addressed in pursuing this model. We have considered the backbone to be topologically entangled with its environment, but the only constraints it sees will be those which decay on time scales comparable to its own, which are those arising from backbones of neighboring H's. On these time scales, all backbone–arm entanglements will have decayed via constraint release. The free arms act as a solvent for the backbones, increasing the effective tube diameter from $a$, which is applicable to the free arms, to $a'$ where

$$a' = a[M_b/(M_b + 4M_a)]^{-1/2} \quad (3)$$

This uses the result, from the behavior of plateau moduli, that $a \sim (\text{concentration})^{-1/2}$.[26] Nevertheless, there is al-

ways a range of molecular weights of backbone ($M_b$) and arm ($M_a$) for which backbone reptation dominates over "tube relaxation".[27] This is considered in more detail in the Appendix.

Second, for melts which relax on realistic time scales, the presence of the branches requires that the ratio $M_b/M_e$ be not greater than 10 or so, whereas linear polymers have been investigated with $M/M_e$ of several hundred. In this limit, path-length fluctuations become unimportant. A polymer in a tube of radius $a$ has an effective potential[26] for its path length of

$$U(L) = \nu kT/na^2(L - na)^2 \quad (4)$$

where $n = (M/M_e)$. The probability distribution for the path length is Gaussian such that

$$\langle \Delta L^2 \rangle / \langle L \rangle^2 \sim n^{-1} \quad (5)$$

Fluctuations become important for small $n$ so they must be taken into account in the H-polymer model. Applying (3) to Roovers polystyrenes,[23] for example, gives his longest backbone extending to about three effective entanglements.

The model contrasts with those of linear and star polymers in that, while both of these can be treated by a distribution function in one variable in the reptative domain,[1] we require two degrees of freedom. These may be thought of as the positions along a primitive path of the two branch points or equivalently as the center of mass and path length of the backbone.

### Linear Viscoelasticity

Under linear deformations, the stress after a step strain is simply proportional to the path length, or number of tube segments surviving that were in existence on application of the strain. We must calculate how the distribution function for this quantity evolves. Readers not interested in the mathematical formulation of the problem are referred to the discussion following the expression for the linear viscosity (eq 17).

We first consider the equation of motion of the distribution function $f$ for the positions of the branch point diffusers $x_1$ and $x_2$. In units where their equilibrium spacing is unity and the elastic force between them $\epsilon$, we can write for $f$ the Smolochowski equation

$$\frac{\partial f}{\partial t'} - \frac{\partial}{\partial x_1'}\left(\frac{\partial f}{\partial x_1'} - \epsilon(x_2' - x_1' - 1)f\right) - \frac{\partial}{\partial x_2'}\left(\frac{\partial f}{\partial x_2'} + \epsilon(x_2' - x_1' - 1)f\right) = 0 \quad (6)$$

The transformation to the primed coordinates is

$$x' = x/na \quad (7a)$$

$$t' = tkT/\zeta n^2 a^2 \quad (7b)$$

$$\epsilon = 2\nu n \quad (7c)$$

We can diagonalize the operator in terms of new coordinates

$$\xi_1 = x_1 + x_2 \quad (8)$$

$$\xi_2 = x_1 - x_2 - 1 \quad (9)$$

when (6) becomes

$$\frac{\partial f}{\partial t} = \frac{\partial^2 f}{\partial \xi_1^2} + \frac{\partial}{\partial \xi_2}\left(\frac{\partial f}{\partial \xi_2} + \epsilon \xi_2 f\right) \quad (10)$$

Now we consider the function $P(\xi_1,\xi_2,\xi_{10},\xi_{20},t,t')$ the probability that a tube segment at the origin exists at time $t$ with diffusers at $\xi_1$ and $\xi_2$ given that their initial values at $t'$ were $\xi_{10}$ and $\xi_{20}$. This must obey the same differential equation as $f$, but we must apply absorbing boundary conditions at the points on the $\xi_1,\xi_2$ plane corresponding to a branch point passing the origin. These boundaries and a contour diagram of the form of the eigenfunction with the lowest eigenvalue are given in Figure 2. The problem as it stands was considered by Doi in his work on path-length fluctuations in linear polymers[28] but not solved, as he wished to find an approximate solution to the multidimensional problem, considering all Rouse modes.

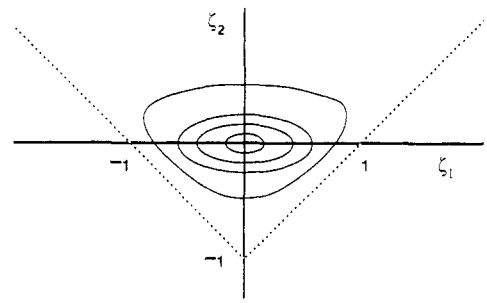


**Figure 2.** Domain and boundaries (dotted) for the partial differential eq 10.

The difficulty of the problem lies in the fact that the operator and boundary conditions cannot simultaneously be diagonalized by any transformation of variable. The operator of (10) has boundary conditions

$$f = 0 \quad \text{on} \quad \xi_1 + \xi_2 = -1 \quad \xi_1 - \xi_2 = 1 \quad (11)$$

and can be made self-adjoint by the weight function

$$f_{eq}(\xi_1,\xi_2) = \exp(-\epsilon\xi_2^2/2) \quad (12)$$

In terms of the eigenfunctions $\phi_n(\xi_1,\xi_2)$ and eigenvalues $\lambda_n$ of the self-adjoint operator, we have

$$P(\xi_1,\xi_2,\xi_{10},\xi_{20},t,t') = \sum_n \phi_n(\xi_1,\xi_2)\phi_n(\xi_{10},\xi_{20}) \exp(-\lambda_n(t - t')) \quad (13)$$

In the high $\epsilon$ limit we note that the problem is not sensitive to the form of the boundary conditions far from the equilibrium value of $\xi_2 = 0$. The eigenfunctions can then be approximated by

$$\phi_{nm}(\xi_1,\xi_2,t) = H_n((2/\epsilon)^{1/2}\xi_2) \exp(-\xi_2^2/\epsilon) \exp(\pm im\pi\xi_1/2) \exp(-\lambda_{nm}t) \quad (14)$$

with

$$\lambda_{nm} = m^2\pi^2/2 + n\epsilon \quad (15)$$

Here the $H_n$ are Hermite polynomials which arise from the $\xi_2$-dependent part of (10) once the boundaries can be approximated by ones parallel to the $\xi_2$ axis. The eigenvalue spectrum reverts as it must to that of a simple relaxed chain in the limit of $\epsilon \to \infty$, but we must expect an imposed deformation to decay with a richer spectrum of decay times when independent branch point fluctuations are added.

In order to treat more realistic values of the elasticity parameter $\epsilon$ properly, eigenfunctions and eigenvalues of the Smolochowski equation (10) were calculated numerically via a discretization and a sparse matrix diagonalization. The stress relaxation upon step strain is of the form

$$G(t) = \sum_n a_n \exp(-\lambda_n t) \quad (16a)$$

with

$$a_n = \left(\int\int f_{eq}\phi_n \, d\xi_1 \, d\xi_2\right)^2 \quad (16b)$$

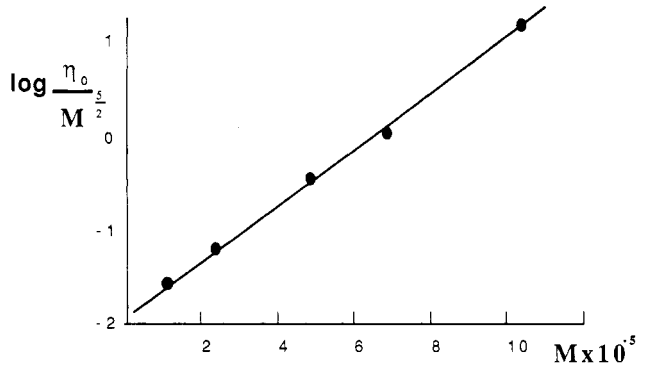


**Figure 3.** log $(\eta_0/M^{5/2})$ against $M \times 10^{-5}$ for Roovers' H-polystyrenes. Here $M = M_a = M_b$.

If there were no path length fluctuations then the viscosity

$$\eta_0 = \int_0^\infty G(t)\, dt \tag{17}$$

of the H-polymers would depend on the square of the backbone molecular weight in contrast to the cubic dependence of linear polymers. This can be seen either by the scaling in (7) or by the following argument. As in tube models of linear and star molecules, we take the stress at time $t$ to be proportional to the amount of occupied tube that has not been passed by a chain end (or in this case by a branch point) by time $t$. For linear polymers $\eta_0 \sim G_p T_d$ where $G_p$ is the plateau modulus and $T_d$ the reptation time characterizing the loss of occupied tube segments. For H-polymers we will have $\eta_0 \sim G_p' T_H$ where $G_p'$ is a diluted plateau modulus dependent only on the ratio $(M_b/M_a)$. If this is a constant (as for Roovers' polystyrenes[23]) then all the dependence on $M_b$ comes from $T_H$. This is the characteristic time for the backbone to reptate (diffuse) out of its tube of length $\sim M_b$ so it will obey $DT_H \sim M_b^2$ with $D$ given by (1). In this case $D$ is only dependent on $M_a$, not on $M_b$ (contrast linear polymers for which $D \sim M^{-1}$ and $T_d \sim M^3$).

For $n$ large this is valid, but particularly for $n < 10$, fluctuations in path length can become important, as Doi[28] has discussed. Around $n = 3$, (17) gives an enhancement to the power law dependence of as much as 0.8 (i.e., $\eta_0 \sim (M_b)^{2.8}$). This comes from the evaluation of (17) as a function of $\epsilon$. An ideal experimental test of this result would be to vary the backbone molecular weight independently of the arms. In Roovers work[23] all sections of the molecule were varied together, but the effect of the backbone can still be isolated. Unlike the case of 4-arm stars,[9] a plot of log $(\eta_0/M_a^{1/2})$ is not linear for the H's, showing the effect of the backbone on the viscosity. When fluctuations are not negligible, we expect for the H's

$$\eta_0 \sim (M_b/M_e)^{2+0.8}(M_a/M_e)^{3/2} \exp(\nu M_a/M_e) \times (M_b/4M_a + M_b)^{-2} \tag{18}$$

The bracketed ratio in (18) comes from the diluting effect of the free arms on the effective modulus of the backbone. The other factors control the characteristic reptation time of the backbone. The term in $M_b^{0.8}$ comes from the fluctuations. For Roovers' H's $M_a = M_b$ so a plot of log $(\eta^0/M_a^{4.3})$ against $M_a$ might be expected to be linear for this range of molecular weights. The best fit for a preexponential power of $M_a$ from his data is 2.5, however (see Figure 3). This is significantly higher than the result for stars[9] $(\eta_0 \sim M_a^{1/2} \exp(\nu M_a/M_b))$, confirming the presence of a backbone effect, but not as large as this theory predicts. As discussed above, H's examined to date have not been very well entangled in the backbone/backbone sense, so experiments with H's of higher $M/M_e$ would be interesting. Fluctuations do, however, tend to increase the power-law dependence of the viscosity (this result and ref 28). We do not comment further on this interesting point, save to notice that that some recent stress relaxation experiments on linear polymers have also failed to observe predicted levels of path length fluctuations.[29]

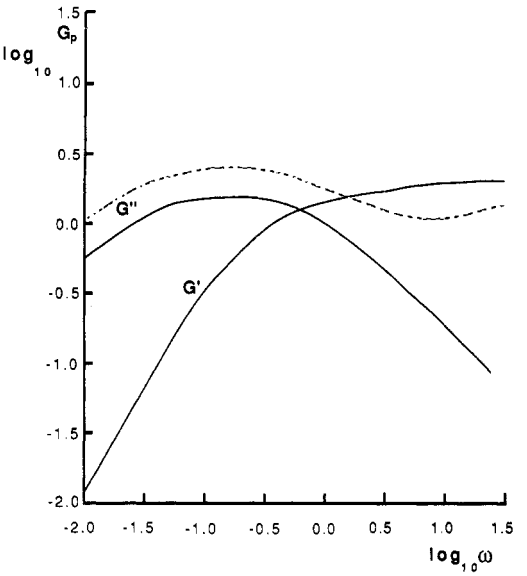


**Figure 4.** Theoretical forms of $G'(\omega)$ and $G''(\omega)$ for the H model with $\epsilon = 2.5$. Normalization is arbitrary, but the high-frequency asymptote of $G'$, when arms also contribute to the stress, is shown. Roovers' results[23] (H5A1) for $G''$ are shown dashed.

A characteristic feature of the linear viscoelasticity of star polymers is that the loss modulus $G''(\omega)$ is monotonic.[9] This is due to the logarithmic form of the stress relaxation in the arms or alternatively the fact that it is not possible to identify any one characteristic time for which the terminal relaxation looks purely exponential. However, in the case of the H's, the relaxation spectrum due to the backbone is a discrete sum of exponentials (16). If the contribution from the arms is ignored this gives

$$G''(\omega) = \sum_n \frac{\lambda_n \omega}{\lambda_n^2 + \omega^2} \tag{19}$$

This function as well as the storage modulus $G'(\omega)$ is given in Figure 4 for a physically interesting value of $\epsilon = 2.5$, corresponding to Roovers' sample H5A1. As the molecular weight of the H polymers is increased, so the contribution of the backbone to the viscoelasticity over the free arms becomes increasingly dominant. We expect a crossover to a loss modulus which exhibits a maximum, and note that this was indeed observed by Roovers.[23] His measurements of $G''(\omega)$ are superposed onto Figure 4, scaled so that the high-frequency plateau value of $G'$ is correct. The dilution effect is a little weaker than predicted by (3), but the form of the low-frequency maximum is well described. The high-frequency turnup to the curve may be attributed to stress contributions from unrelaxed arms. This should have the monotonic form calculated for star arms by Pearson and Helfand.[9]

A final feature of the linear viscoelasticity which shows interesting behavior for branched systems is the recoverable compliance $J_e^0$. For star polymers this is linearly dependent on molecular weight (Rouse-like behavior) as first discussed by Doi and Kuzuu.[8] This is, like the monotonic $G''(\omega)$, due to the nature of the arm relaxation. However, any relaxation spectrum dominated by a sum of discrete exponentials which depend on a characteristic time $\tau$ will give rise to a $J_e^0$ independent of $\tau$ for

$$J_e^0 = \frac{1}{\eta^2}\int^\infty tG(t)\,dt \sim \tau^0 \tag{20}$$

Therefore we expect a crossover behavior with increasing molecular weight from $J_e^0 \sim M$ to $J_e^0 \sim M^0$ if $M_a \propto M_b \propto M$. Roovers does not observe this, although his highest molecular weight H's were still not highly entangled, as has been mentioned above, and the crossover of a property dependent on the integral of the relaxation spectrum will be noticed later than new features in the spectrum itself. It would in any case be interesting to experiment on H's with a higher $M_b/M_e$. The analogous effect in comb polymers has been observed, however, by Roovers and Graessley.[22] These authors comment that when free arms are short compared to the backbone, behavior characteristic of linear polymers rather than stars sets in. This suggests that H's with long backbones will also show it.

### Nonlinear Viscoelasticity

The title of this section is meant in both its senses! As listed in the introduction, long-chain branched polymers in general show interesting features under high deformation rates. Although we neither present a general theory of branched polymer melts here, nor does there exist nonlinear rheological data on H-polymers to date, it is reasonable to suppose that many features of the behavior of randomly branched melts will also appear in the H-melt.

The main additional idea required is the stretching of the backbone at moderate to high deformation rates. This has been treated in the case of linear polymers by Marrucci.[31] In some senses the H-polymer case is simpler because the concentration of effective friction at the branch points means that all parts of the backbone must be equally stretched.

The bulk stress of the material can be calculated from the rubber elastic form used in tube models to date and will take the form

$$\sigma = \frac{3kT\rho}{4\pi a\langle L\rangle^2}\int_0^\infty dL \int d^2\mathbf{u}\; L^2\Psi(L)\Phi(\mathbf{u})(\mathbf{uu} - (1/3)\mathbf{I}) \tag{21}$$

Here $\mathbf{u}$ is the unit vector along a principle path segment, and $\Phi(\mathbf{u})$ is the orientational distribution function for path segments, over which an average is taken. We have made the approximation that the distribution functions for $L$ and $\mathbf{u}$ decouple, which is the case when $\Psi$ is not very broad. Because we will have to consider the cases when the polymer does not have its equilibrium path length, we must also average over the distribution function for path lengths $\Psi(L)$ and weight the tension along the polymer (which in equilibrium is $3kT/a$) accordingly with $L/\langle L\rangle$, where $\langle L\rangle$ is the equilibrium average length. The path-length increase is squared because $L/\langle L\rangle$ more tube segments contribute to the stress while the tension in each tube segment is also greater by $L/\langle L\rangle$.

The problem then becomes one of calculating the distribution functions $\Psi$ and $\Phi$ for an arbitrary flow. The procedure for doing this is described in detail below. The reader not wishing to examine the mathematics should proceed to the following discussion which summarizes and comments on the results.

In the steady state we know that the path-length fluctuations can be treated as the brownian motion of a particle in a one-dimensional harmonic potential. Thus the equation for $\Psi(L,t)$ must be of the form

$$\frac{\partial\Psi}{\partial t} - \frac{1}{\zeta}\frac{\partial}{\partial L}\left(kT\frac{\partial\Psi}{\partial L} + \frac{\Psi\partial U(L)}{\partial L}\right) = 0 \tag{22}$$

where $U(L)$ is the potential for the path length and is

$$U(L) = (\nu kT/na^2)(L - na)^2 \tag{23}$$

Here $L$ corresponds to $\xi_2$ of the last section. The solution of (22) is straightforward and has the eigenvalue spectrum of Hermite's equation and an equilibrium distribution function

$$\Psi_{eq}(L) \sim \exp[-(\nu/na^2)(L - na)^2] \tag{24}$$

We now consider the behavior of $\Psi(L)$ in a flow field described by the deformation rate tensor $\mathbf{g}(t)$ defined in terms of the velocity field $\mathbf{v}(\mathbf{r})$ as

$$g_{ij} = \partial v_i/\partial x_j \tag{25}$$

We make the usual assumption that primitive path segments deform affinely with the flow. In this case the rate of increase in length of all segments of orientation $\mathbf{u}$ will be $(\mathbf{u}\cdot\mathbf{g}\cdot\mathbf{u})\Phi(\mathbf{u})$, which gives an additional current to the time behavior of $\Psi(L)$. Under deformation therefore (22) becomes

$$\frac{\partial\Psi}{\partial t} + \frac{\partial\Psi}{\partial L}(L)L\int d^2\mathbf{u}\;(\mathbf{u}\cdot\mathbf{g}\cdot\mathbf{u})\Phi(\mathbf{u},t) - \frac{1}{\zeta}\frac{\partial}{\partial L}\left(kT\frac{\partial\Psi}{\partial L} + \frac{\Psi\partial U}{\partial L}\right) = 0 \tag{26}$$

So the equations of motion for $\Psi$ and $\Phi$ are coupled. We go on to consider the calculation of $\Phi(\mathbf{u})$ below, but it is clear in general that the solution for most flow histories will require numerical calculation. It is worth pointing out, however, that progress can be made under conditions of steady flow. In this case $\Phi(\mathbf{u})$ is a constant in time and we can put

$$\int d^2\mathbf{u}\;(\mathbf{u}\cdot\mathbf{g}\cdot\mathbf{u})\Phi(\mathbf{u}) = S(K) \tag{27}$$

where $K$ is the shear or extension rate and

$$\partial\Psi/\partial t = 0 \tag{28}$$

in (26). This equation is still soluble and the solution Gaussian in form:

$$\Psi(L,K) \sim \exp\left[-\left(\frac{\nu n}{\langle L\rangle^2} - \frac{S\zeta}{2kT}\right)\times\left(L - \frac{\nu n}{\langle L\rangle^2}\left(\frac{\nu n}{\langle L\rangle^2} - \frac{S\zeta}{kT}\right)^{-1}\langle L\rangle\right)^2\right] \tag{29}$$

The parameter which indicates that $\Psi$ is significantly different from its equilibrium form is therefore $S\zeta\langle L\rangle^2/kTn$, which approaches the ratio of deformation rate to the terminal relaxation time of the molecule for small $n$, which in turn is a condition met by long-chain branched melts.

We now go on to calculate the orientational distribution function $\Phi(\mathbf{u},t)$, following a discussion of linear melts by Marrucci.[31] It is helpful to introduce a restricted distribution function $\Phi(\mathbf{u},t,t')$ which considers only segments created at time $t'$ and still surviving at $t$. If we define the deformation tensor $\mathbf{E}(t,t')$ as

$$E_{ij}(t,t') = \partial x_i(t)/\partial x_j(t') \tag{30}$$

and the vector $\epsilon(\mathbf{u})$ by

$$\epsilon(\mathbf{u}) = \mathbf{E}\cdot\mathbf{u}|\mathbf{E}\cdot\mathbf{u}|^{-1} \tag{31}$$

then the direction of the segment with direction $\mathbf{u}$ at time $t'$ at time $t$ is $\epsilon(\mathbf{u})$, but the value of $\Phi(\mathbf{u})$ will be weighted

at $\epsilon(\mathbf{u})$ in proportion to the length of the segment $|\mathbf{E}(t,t')\cdot\mathbf{u}|$. Therefore

$$\Phi(\mathbf{u},t,t') \sim \int d^2\mathbf{u}'\, |\mathbf{E}(t,t')\cdot\mathbf{u}|\delta(\mathbf{u} - \epsilon(\mathbf{u}')) \qquad (32)$$

Applying the normalization condition that the integral over $\mathbf{u}$ for $\Phi$ be unity gives the constant of proportionality in (32) as $\langle|\mathbf{E}(t,t')\cdot\mathbf{u}|\rangle^{-1}$ where $\langle\ \rangle$ denotes an average over all orientations $\mathbf{u}$.

This leaves the problem of calculating the probability that a tube segment created at time $t'$ (which we assume samples an isotropic distribution) still exists at time $t$. We denote this by $P(t,t')$. This is discussed below, but it is worth noting here that once calculated, all the steady-state components of the stress tensor can be calculated by solving a self-consistent equation for $S$ from (27).

$$S = \int_0^\infty ds \int d^2\mathbf{u}\, \frac{\partial}{\partial s} P(0,-s;S)(\epsilon_s(\mathbf{u})\cdot\mathbf{g}(s)\cdot\epsilon_s(\mathbf{u}))|\mathbf{E}_s\cdot\mathbf{u}|\langle|\mathbf{E}_s\cdot\mathbf{u}|\rangle^{-1} \qquad (33)$$

In the units of the last section we can rewrite (29) with a normalization $N$, as

$$\Psi_{eq} = N \exp[-\tfrac{1}{2}[(\epsilon - S)\xi_2^2]] \qquad (34a)$$

$$Z = (1 - S/\epsilon)^{-1} \qquad (34b)$$

with $\langle x_2 - x_1\rangle$ increased by a scale factor $Z$ from the case where $S = 0$. If we now transform the variables in (6) again by

$$t'' = t'(1 - S/\epsilon)^2 \qquad (35a)$$

$$\xi_1'' = \xi_1'(1 - S/\epsilon) \qquad (35b)$$

$$\xi_2'' = \xi_2'(1 - S/\epsilon) \qquad (35c)$$

Then we regain (6) with its boundary conditions in terms of the new variables except that the elasticity parameter $\epsilon$ becomes

$$\epsilon'' = \epsilon(1 - S/\epsilon)^{-1} \qquad (36)$$

If we define the function $P_0(t,t';\epsilon)$ to be the survival probability function calculated for (6), then for nonzero $S$ (in a flow field)

$$P(t,t';\epsilon,S) = P_0[t(1 - S/\epsilon)^2, t'(1 - S/\epsilon)^2; \epsilon(1 - S/\epsilon)^{-1}] \qquad (37)$$

This allows us to reduce the survival problem for arbitrary $S$ to the single function parameterized by $\epsilon$ that we can calculate from the eigenfunctions of (6). We notice right away that this treatment predicts a strain-rate dependent memory kernal for the stress. Mead and Mackley[32] report a flow away from a constriction where the stress birefringence in a branched melt decays more slowly than in a linear melt, even though their characteristic times are oppositely ordered under linear deformation. It will turn out that this lack of factorizability is important especially in extensional flow.

From the time reversal symmetry of (6), $P_0(t,t')$ is also the probability that a segment at $(\xi_0,t')$ is destroyed at $t$. We have

$$P_0(t,t';\epsilon) = \int\int\int\int d\xi_{10}\, d\xi_{20}\, d\xi_1\, d\xi_2\, (\partial P/\partial t')(\xi_1,\xi_2,\xi_{10},\xi_{20},t,t';\epsilon) \qquad (38)$$

For the following we adopt a terminal time approximation for $P_0(t,t';\epsilon)$. The extension to a full spectrum of relaxation times is straightforward but only changes details.

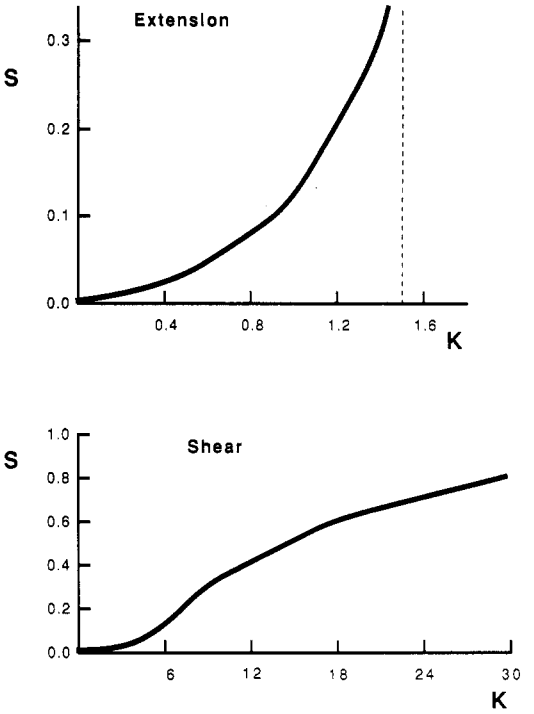


**Figure 5.** Orientational integral $S$ as a function of deformation rate $K$ in both shear and extension.

From the numerical calculation we find that over $1 < \epsilon < 5$, which is a relevant range experimentally, $P_0(t,t';\epsilon)$ is well approximated by

$$P_0(t,t';\epsilon) \cong \exp[-(1 - 1/2\epsilon)(t - t')] \qquad (39)$$

This explicit form permits us to solve for $S(K)$ in (33). In simple shear (33) takes the form

$$S(K) = \int_0^\infty dt\, \frac{KF_4(Kt)}{F_5(Kt)} \exp[-(1 + (1 - S/\epsilon)/2\epsilon)(1 - S/\epsilon)^2 t] \qquad (40)$$

where

$$F_4(\lambda) = \langle (u_x + \lambda u_y)(1 + 2\lambda u_x u_y + \lambda^2 u_y^2)^{-1/2}\rangle \qquad (41)$$

and

$$F_5(\lambda) = \langle (1 + 2\lambda u_x u_y + \lambda^2 u_y^2)^{1/2}\rangle \qquad (42)$$

$\langle\ \rangle$ denotes an angular average over the unit sphere. To take an interesting specific case, we take $\epsilon = 1$ (corresponding to $n \cong 2$). This can be solved numerically by an iterative routine, but in fact in shear $S(K)$ is quite a weak function. Writing it as an expansion,

$$S(K) = a_2K^2 + a_4K^4 + \ldots \qquad (43)$$

and doing the angular integrals and the time integral in (40) give

$$a_2 = 3.4 \times 10^{-2} \qquad a_4 = -2.1 \times 10^{-2}$$

(in shear for $\epsilon = 1$)

From the expression for the average path length (34b) we note that the stress diverges under our present assumptions if $S = \epsilon = 1$. For this value and larger values of $\epsilon$ in shear flow, this point is not reached until large shear gradients on the order of 10 are achieved. For these values of $K$ (40) must be solved numerically. The result is presented in Figure 5. Only a very small rise in viscosity is predicted before shear thinning occurs as for a linear melt, which is shown in Figure 6 with the elongational viscosity.

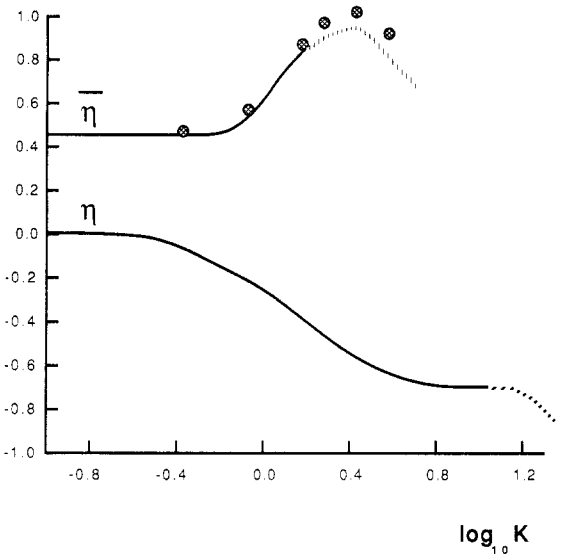


**Figure 6.** Theoretical curves of the extensional and shear viscosities as functions of deformation rate $K$. Points are scaled results of Meissner in extension. Dashed lines show the effect of the onset of arm retraction.

The situation is quite different in extension, when (33) becomes

$$S(K) = \int_0^\infty dt\, K f_{st}[\exp(Kt)] \exp[-\tfrac{1}{2}(3 - S)(1 - S)^2] \tag{44}$$

with $f_{st}$ as given in ref 2. It is a function which at the origin is zero but has a positive gradient and tends smoothly to a constant positive value for large values of the argument. Because of the exponential dependence of deformation on time in steady elongational flow, the function $S(K)$ within this theory may diverge at finite $K$ if the integral becomes undefined. Numerical evaluation of the function is presented in Figure 5.

## Discussion of Nonlinear Behavior

In the treatment presented above, we found that the stress in an H-polymer melt can be calculated in the nonlinear flow regime. For steady flow, a rescaling of the linear diffusion problem self-consistently and dependent on the deformation rate led to an expression for the stress permitting an extension of the primitive path length of the backbone. This physical process, which is more important in multiply branched polymers than in linear polymers, has a number of consequences.

First, we lose time/strain factorization except in the limit of very high molecular weight.

Second, we can calculate the steady-state stress tensor in both shear and elongation and derive from this the nominal viscosities as functions of deformation rate. These are plotted in Figure 6 for the case where $\epsilon = 1$ (which would correspond physically to Roovers' sample H3A1). We observe very different response in shear and extension. The H-melt is, like a linear polymer, still shear thinning though not as strongly so at high shear rates. This is consistent with experiments on multiply branched LDPE (see, e.g., Wales[30]). In extension we predict deformation-thickening or an upturn in viscosity with shear rate. Though not in any way intended as a direct quantitative comparison, the experiments of Meissner[12] on branched LDPE are superimposed. It would be very interesting to test this effect with a well-characterized H-melt, when a more quantitative comparison with the model could be made.

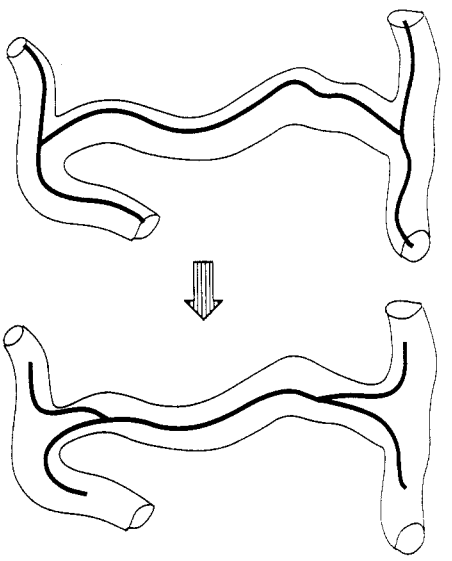

**Figure 7.** Proposed collapse of the H-polymer under high strains.

Third, we note that the stress/shear rate curve for this model is monotonic, unlike that of linear polymers. This suggests why discontinuities in capillary flow are not seen in branched polymers.[7,17]

Fourth, in both shear and extension there exist critical deformation rates at which the model is ill-defined, and no steady-state conformation of the H-polymer can be found. This corresponds to infinite extension of the backbone which is clearly unphysical. At the point of divergence or before, some new physical process must become important. One possible solution, which does not require going beyond a Gaussian model for the polymer chains, is discussed in the next section.

## Critical Deformation Levels

The physical process which prevents divergence in the stress must relate to a change in the effective diffusion constant of the branch points. As pointed out by R. C. Ball[33] the free arms cannot support arbitrarily large extension of the backbone and will be dragged into its tube (Figure 7). This can also be expected to occur in step strain when the backbone becomes sufficiently stretched to make it entropically favorable to reduce its length, paying the penalty of requiring a length of a doubly occupied tube.

The simplest way to think about these entropies is to consider the effective tensions in an entangled chain which result. In a segment of polymer that has its equilibrium path length, the tension is

$$f_{eq} = 3kT/a \tag{45}$$

For a segment of a polymer whose path length has been increased to $\langle|\mathbf{E}\cdot\mathbf{u}|\rangle$ by a deformation $\mathbf{E}$, the tension is

$$f' = f_{eq}\langle|\mathbf{E}\cdot\mathbf{u}|\rangle \tag{46}$$

In order for the process in Figure 7 to occur, the equilibrium tensions in the two free arms when summed must be equal to or less than the single tension in the backbone

$$2f_{eq} \leq f_{eq}\langle|\mathbf{E}\cdot\mathbf{u}|\rangle \tag{47a}$$

so

$$\langle|\mathbf{E}\cdot\mathbf{u}|\rangle > 2 \tag{47b}$$

For a general branched polymer of total arm molecular weight $M_a$ and backbone molecular weight $M_b$ we must weight the arm contribution to the stress (with equilibrated

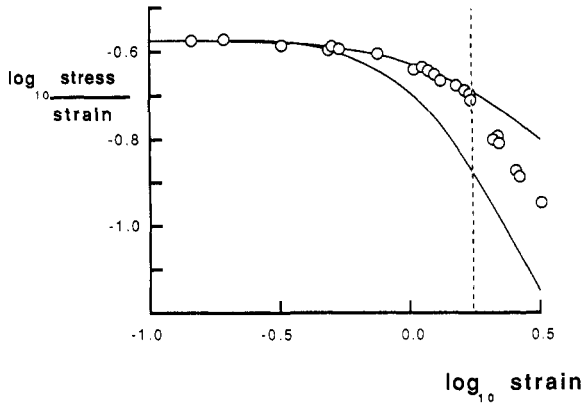


**Figure 8.** Results of Kimura et al. on step shear strain of branched polyethylene. The quantity plotted is log (stress/strain). The theoretical curve of (48) is superimposed. The lower curve is the Doi–Edwards result for a linear melt. The dashed line indicates where max ($|\mathbf{E}\cdot\mathbf{u}|$) = 2.

path length and tension) by $M_a/(M_a + M_b)$ and the backbone contribution (nonequilibrated path length and tension) by $M_b/(M_a + M_b)$. This gives, for times intermediate between arm relaxation and backbone reptation:

$$\sigma = \langle \mathbf{E}\cdot\mathbf{u}\mathbf{E}\cdot\mathbf{u}(|\mathbf{E}\cdot\mathbf{u}|)^{-1}\rangle[\langle|\mathbf{E}\cdot\mathbf{u}|\rangle M_b/(M_a + M_b) + \langle|\mathbf{E}\cdot\mathbf{u}|\rangle^{-1}M_a/(M_a + M_b)] \quad \text{for } \langle|\mathbf{E}\cdot\mathbf{u}|\rangle < 2$$

$$\sigma = \langle \mathbf{E}\cdot\mathbf{u}\mathbf{E}\cdot\mathbf{u}(|\mathbf{E}\cdot\mathbf{u}|)^{-1}\rangle\langle|\mathbf{E}\cdot\mathbf{u}|\rangle^{-1}(M_a + 4M_b)/(M_a + M_b) \quad \text{for } \langle|\mathbf{E}\cdot\mathbf{u}|\rangle > 2 \quad (48)$$

The stress/strain curve is continuous but has a discontinuous gradient. Kimura et al.[15] have done a step strain experiment in shear on a randomly branched polyethylene with known branch-point and end-group probabilities. Their results are replotted in Figure 8 together with the theoretical curve of (48). The discontinuity in the gradient does appear, and up to that point the data fit the curve well. However, the discontinuity occurs at a smaller strain than expected. This might be due to very short sections of backbone, since this point is experimentally at the strain where max ($|\mathbf{E}\cdot\mathbf{u}|$) = 2 rather than $\langle|\mathbf{E}\cdot\mathbf{u}|\rangle$ itself, or due to residual nonequilibrated backbones, as the backbone reptation time would have been very long for their sample.

In steady flow the analogous effect will occur. By adopting the configuration of Figure 7 on average, an H-polymer can reduce its backbone reptation time even though its path length is increased, because the diffusion of the new effective "branch points" is exponentially faster. This decreases the effective deformation rate $K$ in (44) to a value that keeps $S$ below the point of divergence. The detailed treatment of this effect will be the subject of future work, though the onset of the effect is shown by the dashed portion of the curves in Figure 6.

## Conclusion

The model of the H-polymer which concentrates on the dynamics and environment of the backbone allows the calculation of linear and nonlinear viscoelastic properties. The idea of a confining tube and primitive path generalizes naturally from the case of linear polymers.

A number of features observed experimentally are explained by the model, though the loss of molecular weight dependence of $J_e^0$ with longer backbones has yet to be seen, and there are indications that fluctuations in path length may not be as strong as expected, insofar as they affect stress decay.

Particularly striking is the strain hardening in nonlinear elongational flow which is qualitatively different from the behavior of linear polymers.

We predict critical levels of deformation at which a conformational change occurs, effectively shortening the free arms. This may already have been observed in step strain experiments.

The unusual flow field mentioned in the introduction is clearly related to the behavior in extension. We are now in a position to examine this in detail. It is also hoped to extend this work to the case of randomly or multiply branched polymers.

Experiments on the nonlinear viscoelasticity of well-characterized branched polymers are awaited with interest.

**Acknowledgment.** I thank Dr. R. C. Ball, Prof. Sir Sam Edwards, Dr. M. E. Cates, W. Barford, D. Agg, and D. Mead for useful discussions. The work was supported by a CASE studentship with the SERC (UK) and Courtaulds plc.

## Appendix

We need to show that, for high enough molecular weight, the reptative motion of the H backbone will dominate over other large-scale diffusive processes, such as tube reorganization.

To calculate the latter we use a Rouse-like dynamics of the tube depending on the lifetime of an entanglement (see, e.g., Klein[25]) $\tau_{ent}$.

For the reptation time

$$\tau_{rept} \sim (\text{primitive path length})^2/D \sim a^2(M_b/a^2)^2(M_a/M_e)^{3/2}\exp[-\nu(M_a/M_e)] \sim M_b^2[M_b/(4M_a + M_b)](M_a/M_e)^{3/2} \times \exp[-\nu(M_a/M_e)]$$

since $a^2 \sim M_e$ and $a \sim (\text{density})^{-1/2} \sim (M_b/(4M_a + M_b))^{-1/2}$.

For the Rouse relaxation of the tube,

$$\tau_{tube} \sim (\text{p.p length})^2\tau_{ent} \sim M_b^2[M_b/(4M_a + M_b)]\tau_{rept} \quad \text{if } \tau_{rept} \sim \tau_{ent}$$

So $\tau_{tube}/\tau_{rept} \sim M_b^3/(4M_a + M_b) \sim M^2$ if $M_a = M_b = M$. So as $M$ increases at fixed monomeric concentration, the backbone reptation dominates.

## References and Notes

(1) Doi, M.; Edwards, S. F. *J. Chem. Soc., Faraday Trans. 2* **1978**, *74*, 1789.
(2) Doi, M.; Edwards, S. F. *J. Chem. Soc., Faraday Trans. 2* **1978**, *74*, 1802.
(3) Doi, M.; Edwards, S. F. *J. Chem. Soc., Faraday Trans. 2* **1978**, *74*, 1818.
(4) Doi, M.; Edwards, S. F. *J. Chem. Soc., Faraday Trans. 2* **1979**, *75*, 38.
(5) Osaki, K.; Kurata, M. *Macromolecules* **1980**, *13*, 671.
(6) Marrucci, G. *J. Non-Newtonian Fluid Mech.* **1987**, *21*, 319.
(7) McLeish, T. C. B.; Ball, R. C. *J. Polym. Sci., Part B* **1986**, *24*, 1735.
(8) Doi, M.; Kuzuu, N. *J. Polym. Sci., Polym. Lett. Ed.* **1980**, *18*, 775.
(9) Pearson, D. S.; Helfand, E. *Macromolecules* **1984**, *17*, 888.
(10) Needs, R. J.; Edwards, S. F. *Macromolecules* **1983**, *16*, 1492.
(11) Klein, J., et al. *Faraday Symp. Chem. Soc.* **1983**, *18*, 159.
(12) Meissner, J. *Rheol. Acta* **1971**, *10*, 230.
(13) Laun, H. M.; Muenstedt, H. *Rheol. Acta* **1976**, *15*, 517.
(14) Blyler, L. L. *Rubber Chem. Technol.* **1968**, *41*, 823.
(15) Kimura, M.; et al. *J. Polym. Sci., Part B* **1981**, *19*, 151.
(16) Valles, E. M.; Macosco, C. W. *Macromolecules* **1979**, *12*, 521.
(17) den Otter, J. L. *Rheol. Acta* **1971**, *10*, 200.
(18) Bialas, G. A.; White, J. L. *Rubber Chem. Technol.* **1969**, *42*, 682.
(19) Ballenger, T. F.; White, J. L. *J. Appl. Polym. Sci.* **1971**, *15*, 1949.
(20) Graessley, W. W. *Adv. Polym. Sci.* **1982**, *47*, 67.
(21) Pearson, D. S.; Helfand, E. *Faraday Symp. Chem. Soc.* **1983**, *18*, 189.
(22) Roovers, J.; Graessley, W. W. *Macromolecules* **1981**, *14*, 776.

(23) Roovers, J. *Macromolecules* **1984**, *17*, 1196.
(24) Marrucci, G. In *Advances in Transport Processes*; Mujumdar, A. S., Mashelkar, R. A., Eds.; Wiley: New York, 1984; Vol. 4.
(25) Klein, J. *Macromolecules* **1986**, *19*, 105.
(26) Doi, M.; Edwards, S. F. *The Theory of Polymer Dynamics*; Oxford: 1986.
(27) Viovy, J. L., et al. *J. Polym. Sci., Part B* **1983**, *21*, 2427.
(28) Doi, M. *J. Polym. Sci., Part B* **1983**, *21*, 667.
(29) Tassin, J. F. Thesis, University of Paris VI, 1986.
(30) Wales, J. L. S. *The Application of Flow Birefringence to Rheological Studies of Polymer Melts*; Delft: 1976.
(31) Marrucci, G., submitted to *J. Non Newtonian Fluid Mech.*
(32) Mackley, M.; Mead, D., unpublished results.
(33) Ball, R. C., private communication.
(34) Cogswell, F. N. *Polymer Melt Rheology: A Guide for Industrial Practice*; Goodwin: London, 1981.

# Effect of Elongational Flow on Polymer Adsorption

**G. J. Besio,† R. K. Prud'homme,* and J. B. Benziger**

*Princeton University, Department of Chemical Engineering, Princeton, New Jersey 08544.*
*Received May 28, 1987; Revised Manuscript Received October 6, 1987*

ABSTRACT: The adsorption and desorption of polystyrene (PS) from cyclohexane at 34.8 °C (θ temperature) on a chrome mirror has been studied by using ellipsometry. Static adsorption measurements give adsorbed layer thickness and adsorbed amounts in agreement with previous investigators. The effect of elongational flow on polymer adsorption and desorption was studied by directing a jet of polymer solution or solvent perpendicular to the mirror surface, to produce an elongational velocity field at the stagnation point on the surface. For a $10^7$ $M_w$ PS adsorbed under strong elongational flow conditions, the adsorbed layer was an order of magnitude thinner than a layer adsorbed under quiescent conditions and the polymer concentration in the layer adsorbed under elongational flow was 3.4 times higher. The effect of elongational flow of solvent on the desorption of a polymer layer formed under quiescent conditions was studied. No desorption was observed at the stagnation point. The impinging solvent jet produced a distinctive pattern on the chrome mirror in the desorption experiments. A "bull's-eye" pattern was visible on the dried mirror, showing a center circle of adsorbed polymer, a clear annular ring where shear forces desorbed the polymer, and a region of adsorbed polymer out beyond the desorbed ring.

## Introduction

Polymer adsorption from flowing solutions is important in applications such as enhanced oil recovery, pigment dispersion, and flow-enhanced flocculation. The effect of flow conditions on polymer adsorption has received little attention, because it is difficult to impose a controlled flow field while simultaneously monitoring adsorption. Notable exceptions are recent studies by Robertson,[1,2] using attenuated total reflection spectroscopy (ATR), and Fuller,[3,4] using ellipsometry to study adsorption in shear flow.

Shear flows produce small changes in molecular conformation in dilute solution, whereas elongational flows can produce large conformational changes. In elongational flow fields, when the elongational strain rate, $\dot{\epsilon}$, exceeds the relaxation time of the polymer molecule, $\tau$, the molecule undergoes a coil–stretch transition and becomes highly elongated.[5-7] The coil–stretch transition in an elongational flow field has been directly observed in crossed-flow birefringence by Keller who inferred from the difficulty in cleaning his apparatus that polystyrene sulfonate adsorbed irreversibly when adsorbed from a solution in a stretched state.[5] However, there was no direct evidence as to the nature of the polymer layer adsorbed under stretched-state conditions. In this paper we report an ellipsometric study of polystyrene adsorption in an elongational flow, produced by an impinging jet.

## Polystyrene Adsorption

**A. Summary of Static Experiments.** A comprehensive study of the adsorption of polystyrene was carried out by Takahashi and co-workers[8] who studied the adsorption of polystyrene of molecular weights ranging from 10 000 to 13 000 000 onto chrome from cyclohexane at the θ temperature (34.8 °C). From these studies, the following trends were observed: (1) the thickness of the adsorbed layer scales with molecular weight to the $^1/_2$ power at low molecular weight, (2) above a molecular weight of 300 000 the surface concentration reaches a plateau at about ~5.0 mg/m$^2$, and (3) the surface concentration is independent of solution concentration above a solution concentration of approximately 1000 ppm.

By monitoring the thickness and refractive index of the adsorbed layer at sequential time steps. Takahashi was able to determine approximate adsorption kinetics. The thickness of the adsorbed layer was found to reach a value close to 80% of its equilibrium value within minutes, however, it took approximately 2–3 h to reach a steady-state value. The surface concentration, $A$, was calculated by $A = (n_f - n_m)\delta/(dn/dc)$, where $\delta$ is the thickness of the adsorbed layer, $n_f$ is the refractive index of the adsorbed layer, $n_m$ is the refractive index of the surrounding medium, and $dn/dc$ is the refractive index increment.

**B. Influence of Shear Flow.** Fuller and Lee[3,4] studied two different effects of flow on adsorption with ellipsometry. In the first experiment, a preadsorbed polymer layer was subjected to a shear flow of pure solvent resulting in "flow-enhanced desorption". In a second experiment, adsorption was carried out from a flowing solution resulting in "flow-inhibited adsorption".

Fuller and Lee found that substantial desorption was induced by shear flow. The desorption was initially rapid, becoming negligible after 30 to 40 min. The amount desorbed increased with increasing shear rate for all polymers and also increased with increasing molecular weight. Interestingly, the thickness of the adsorbed layer was not greatly influenced by the flow-induced desorption, except at the highest molecular weight, indicating that little conformational change was induced in the adsorbed layer by flow.

† Current address: General Electric CRD, P. O. Box 8, Building K-1, 4B33, Schenectady, NY 12301.

0024-9297/88/2221-1070$01.50/0 